Nanoscale

Accepted Manuscript

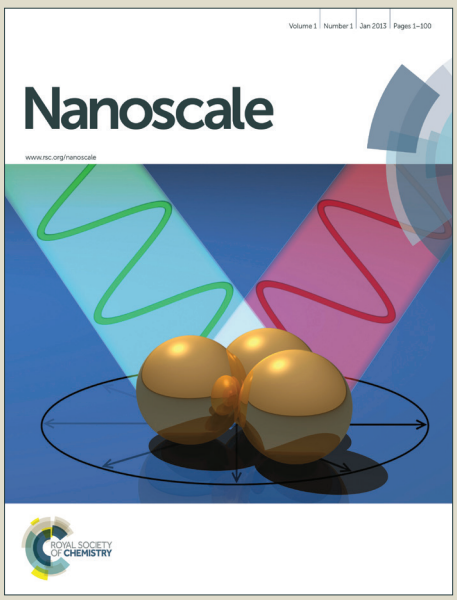

ROYAL SOCIETY OF CHEMISTRY

www.rsc.org/nanoscale

Journal Name

RSCPublishing

COMMUNICATION

Manipulating Directional Cell Motility Using Intracellular Superparamagnetic Nanoparticles

Cite this: DOI: 10.1039/xoxxoooooox

Michael Bradshaw[a,b], Tristan Clemons[a,b], Diwei Ho[a], Lucía Gutiérrez[c,d], Francisco J. Lázaro[e], Michael J. House[c], Timothy G. St. Pierre[c], Mark W. Fear[b,f], Fiona M. Wood[b,f,g] and K. Swaminathan Iyer[a*]

Received ooth January 2014,
Accepted ooth January 2014

DOI: 10.1039/xoxxoooooox

www.rsc.org/

This study investigated the ability for magnetic nanoparticles to influence cellular migration in the presence of an external magnetic field. We found that the direction of migrating keratinocytes can be controlled and the migration speed of fibroblasts can be increased with the internalisation of these nanoparticles in the presence of a magnetic field. The possibility of shepherding cells towards a region of interest through the use of internalized nanoparticles is an attractive prospect for cell tracking, cell therapies, and tissue engineering applications.

Skin injury triggers a cascade of events which mediates tissue repair for the re-establishment of the barrier function. This tissue repair is categorized into an inflammatory phase, a granulation phase with epithelial wound closure, and a scar-remodeling phase.[1] Because skin serves as a protective barrier, any injury to it should be rapidly and efficiently healed. An important fundamental process that dictates efficient wound closure is cell migration.[2] Polarized intracellular signaling orients the protruding leading edge of a migrating cell, integrins mediate adhesion to the underlying substrate, and contraction and detachment at distinct regions of the cell orchestrate cell motility during wound healing.[3, 4] Random migration of a cell occurs when a cell possesses relatively low intrinsic directionality. However, cells undergo directed migration in the presence of motogenic stimuli as an external guidance cue.[5] This steering or compass mechanism coupled to the basic motility machinery has been exploited in the presence of an asymmetric environmental factor to program directional cell migration.[6] It has been well established that cells undergo chemotaxis in response to soluble cues, haptotaxis in response to graded adhesion in the underlying substrate, electrotaxis in response to electric fields, and durotaxis in response to mechanical signals in the environment.[7, 8]

Importantly in the case of skin, deep burn injuries cause destruction of the epidermis and most of the dermis, with few epithelial cells surviving.[9] Following injury, re- epithelialization occurs from the migration of epithelial cells from any remaining epidermal appendages and from the wound margins, but healing does not occur for weeks post injury. The result is a very thin and potentially non-functional epidermis. Within hours after a wound, keratinocytes at the margins of the wound and within hair follicles and glands enter a migratory mode and begin to migrate laterally across the wound bed.[10] How quickly these cells cover the wound bed is critical to how effectively the wound will heal. Until the entire wound bed is resurfaced, the only epithelial cells to proliferate are at the wound edges – migration is crucial at this early stage. Fibroblasts lay down the temporary extracellular matrix during wound healing and produce collagen to help rebuild the skin. However fibroblasts first need to migrate into the wound through the fibrin clot, in order to start re-establishment of the skin.[11] Importantly it is also now widely accepted that crosstalk between epidermal cells (keratinocytes) and the primary cells of the dermis (fibroblasts) is critical to successful wound healing.[12, 13]

Previously it has been shown that cell-internalized superparamagnetic nanoparticles can modulate endosome movement with the aid of an external magnetic field such that the endosomes will chain in the direction of the applied field.[14] The magnetic nanoparticles enclosed in the endosomes give the cells a magnetic moment when in the presence of a magnetic field. Magnetic endosomes behave as small magnets and attract each other *via* dipole-dipole interactions, forming small chains in the cell cytoplasm. Furthermore, it has also been shown cell-internalized magnetic nanoparticles can exert a tensile force inside neurons and axons, stimulating neurite and axon elongation in a particular direction.[15] More recently, it has been reported that labelling mesenchymal stem cells with magnetic nanoparticles and exposing them to a magnetic field (0.6 T) causes the cells to grow along the magnetic flux lines.[16] The two important migratory components of re-epithelialization involve the forward leap of the keratinocytes across the wound bed and the three dimensional migration of fibroblasts to lay down the collagen in the extracellular matrix.[17] In the current study we demonstrate that in the presence of an external magnetic field, intracellular superparamagnetic nanoparticles act as guides to direct the forward leap in the case of keratinocytes and increase three dimensional migration speed in the case of fibroblasts (Fig. 1).

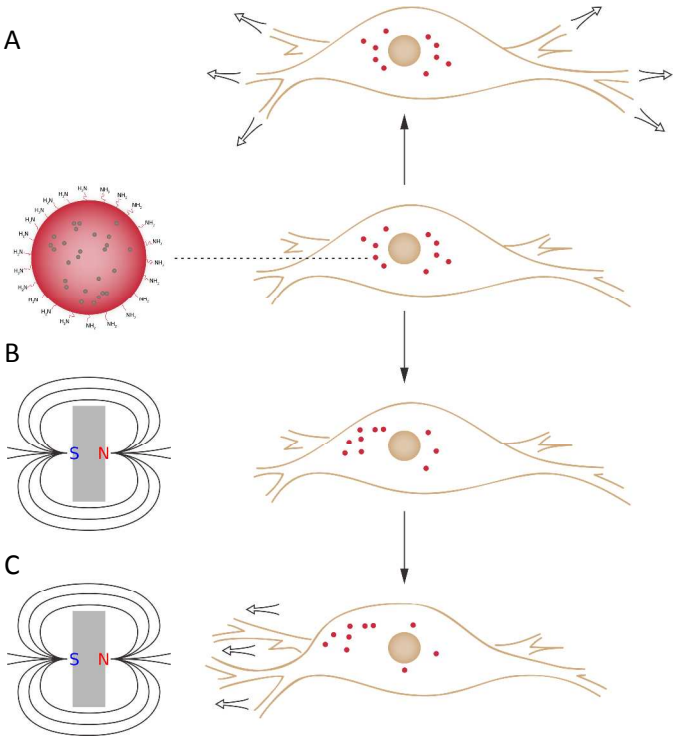

Fig. 1 Schematic representation depicting the ability for an external magnetic field to attract magnetic nanoparticles which have been internalised within cells and in doing so provide migratory cues to the cell to travel in the direction of the external field. (A) Cells with internalized magnetic nanoparticles but without an external magnetic field are free to migrate in all directions. (B) In the presence of an external magnetic field we hypothesise first the attraction of the internalised nanoparticles within the cells which in turn results in (C) migratory cues for the cell in accordance with the applied field.

Iron oxide (magnetite, Fe_3O_4) nanoparticles were encapsulated within polymeric nanoparticles, forming a multicore structure, prepared from a Rhodamine B modified polyglycidyl methacrylate (PGMA) polymer *via* an emulsion synthesis method (Fig. S1, ESI†). The surfaces of these nanoparticles were further modified through the attachment of the cationic polymer, polyethylenimine (PEI) to produce a positive surface on the nanoparticles suitable for cellular internalization. These nanoparticles have previously been used in a range of studies; *in vitro*[18], *ex vivo*[19] and *in vivo*[20] without any significant toxicity or issues found with nanoparticle biocompatibility. The apparent low toxicity coupled with the nanoparticle fluorescent imaging capabilities and ability to achieve rapid cellular internalization in a range of cell lines make this nanoparticle construct an ideal candidate for application in the treatment of burns wounds.

MTS (colorimetric cell viability assay) was used to assess the nanoparticle effects on cellular proliferation of both HaCaT keratinocytes and NIH-3T3 fibroblasts. Application of the nanoparticles did not induce any significant inhibition of cellular proliferation or apparent toxicity for either cell line over a 24 hour time period as assessed by MTS (Fig. S2, ESI†). This biocompatibility was even evident at a maximum nanoparticle concentration of 200 μg ml^{-1}, 4-fold higher than the nanoparticle concentration (50 μg ml^{-1}) used for all further downstream experiments demonstrating cellular magnetic manoeuvrability.

Cellular uptake of the nanoparticles was firstly assessed using live time-lapse confocal microscopy. It was clearly evident that for both the NIH-3T3 and HaCaT keratinocytes that cellular association of the nanoparticles is rapid (within 20 minutes) which results in high amounts of cellular uptake after 11 h (t=660 min) of nanoparticle incubation with the cells (Fig. 2A and B). For further details showing how the nanoparticles are trafficked within the cells, see the attached videos of the 16 h time lapse in the electronic supplementary information for both NIH-3T3 and HaCaT cells. Transmission electron microscopy was also performed with primary dermal fibroblasts and the nanoparticles were clearly seen internalised surrounding the nucleus (Fig. S7, ESI†).

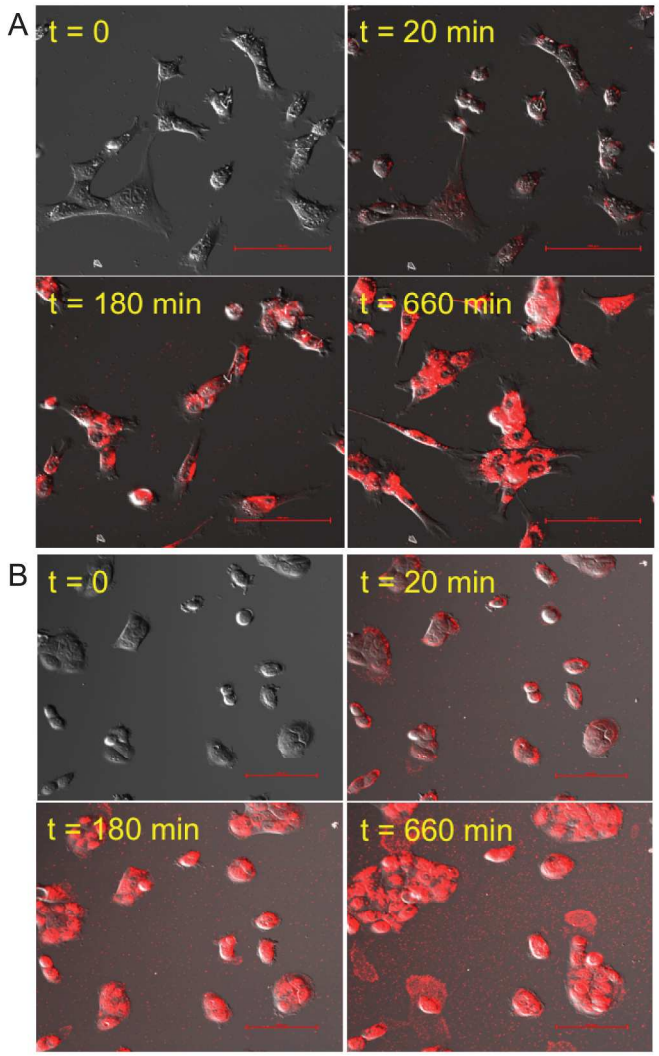

Fig. 2 Live cell confocal time slices of (A) NIH-3T3 cells and (B) HaCaT cells during magnetic nanoparticle uptake. Images were taken every 15 seconds for the first 15 minutes after adding the nanoparticles and then every 10 minutes for 16 hours.

Quantitative analysis of the nanoparticle-cell uptake was measured in both HaCaTs and NIH-3T3 fibroblasts by alternating current (AC) magnetic susceptibility measurements. Both cell types were incubated either with or without nanoparticles for a period of 24 hours, before washing to remove non-internalised nanoparticles and measurements could be made. Although previous studies have shown significant uptake of these nanoparticles within the first hours

of incubation in different cell lines[18, 19] a 24 hour time period was chosen to achieve cell saturation with the nanoparticles. Nanoparticles at different concentrations were prepared in suspensions of low temperature gelling agar suspensions to be used as standards for the magnetic quantification, following previously described protocols.[21] The cells incubated with the nanoparticles and the nanoparticle suspension in agar exhibited a single peak in both the in-phase (χ') and out-of-phase (χ'') susceptibility components, indicative of a magnetic relaxation phenomenon typical of the magnetic nanoparticles.[22] The profile shape of the out-of-phase susceptibility maxima, located at around 35 K, for both cell lines incubated with the nanoparticles and the agar nanoparticle standard solution of 8.50 mg Fe/g, were in tight agreement (Fig. 3A). This strong correlation of fit suggests the magnetic nanoparticles are extremely stable and intact throughout the cellular uptake process in both cell lines tested over a 24 h time period. This similarity allows the magnetic quantification of the particles in the cells taking the magnetic data per mass of iron in the agar gel as a reference. The presence of superparamagnetic nanoparticles in both cell lines is additionally confirmed by comparison with the control cells (without nanoparticles), where the control cells show no out-of-phase susceptibility, in comparison to cells with nanoparticles portraying a single, defined peak (Fig. 3B and 3C).

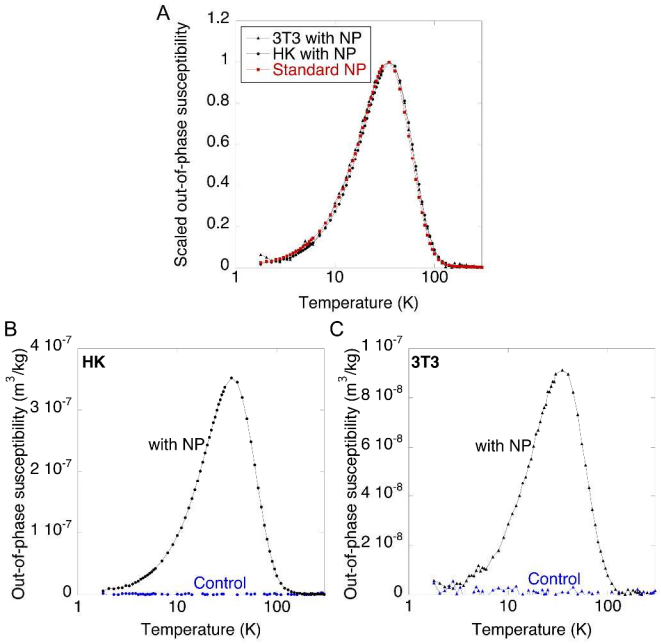

Fig. 3 (A) Temperature dependence of the out-of-phase susceptibility scaled to its maximum for both HaCaT (HK) and NIH-3T3 (3T3) cells incubated with nanoparticles and a standard concentration of the nanoparticle/agar suspension (shown in red). Temperature dependence of the out-of-phase susceptibility for control cells and cells incubated with nanoparticles from two cell lines, (B) HaCaTs and (C) NIH-3T3 fibroblasts.

The iron concentration in the form of particles in each cell line has been calculated following a previously described protocol for magnetic quantification based on AC magnetic susceptibility measurements.[22-24] In brief, the out-of-phase mass specific susceptibility profile of the cells is fitted to the out-of-phase iron specific susceptibility profile of a standard corresponding to the nanoparticles in a non-aggregated state. The multiplication factor obtained for the best fit informs us of the iron concentration in the form of magnetic nanoparticles (Table 1). Based on the magnetic susceptibility measurements it is evident that the HaCaT cells accumulated approximately 4 times more nanoparticles when compared to the fibroblast samples. This was further confirmed by ICP-AES to determine the total iron content on all samples (cells with and without nanoparticles), where the results clearly indicate the cells incubated with the magnetic nanoparticles had accumulated an increase in iron which was comparable with the increase predicted by magnetic susceptibility measurements (Table 1).

Table 1. Quantification of nanoparticle uptake through assessment of iron content in cells following 24h incubation with nanoparticles

Sample	$[Fe]_{MNP}$ (mg/g) magnetic susceptibility analysis	$[Fe]_{TOTAL}$ (mg/g) ICP-AES measurements
HaCaTs control	-	0.203
NIH-3T3 control	-	0.329
HaCaTs with NPs	1.17	1.492
NIH-3T3 with NPs	0.420	0.420

It has been shown that cell-internalised magnetic nanoparticles can exert a tensile force inside neurons and axons, stimulating neurite and axon elongation in a particular direction.[15] Enhanced nerve regeneration was attempted by exploiting the mechanical forces that act on neurons with magnetic nanoparticles. Such a mechanical directing force does not occur naturally in the skin, hence our aim to artificially induce this directed cell migration in populations of skin cells. A previous study has shown that fibroblasts can be polarised with an 8 T magnetic field, by inducing anisotropy using the inherent diamagnetic nature of cells.[25] Although sound proof-of-concept, the practicality of using such a strong magnetic field limits the applicability of this technique. Similar analysis of diamagnetism has been performed on paramecia in a more practical field (0.78 T) and it was found that the cilia and trichocysts are important for the orientation of the protozoa in magnetic fields.[26] Hence for this work, it was hypothesised that through the internalisation of the magnetic nanoparticles in skin cells that we could direct cell migration through the assistance of an external magnetic field.

Keratinocytes such as HaCaTs are found within the epidermal layer of the skin. Following an injury to the skin such as a burn, rapid coverage of the wound with viable cells is integral to minimising scarring and long term damage. Hence, in the case of keratinocytes, 2D migration to mimic coverage of a wound *in vitro* is desirable. To assess this, HaCaT keratinocytes were grown to near confluence on coverslips and then incubated with the magnetic nanoparticles for 24 hours. Following incubation the cells were rinsed and transferred to a new well adjacent to the permanent magnet, where they were incubated for a further 4 days in the presence of the external magnetic field (See Fig S3A ESI† for experimental setup). It was evident from both bright field analysis and fluorescent analysis that the presence of the internalised magnetic nanoparticles in an external magnetic field had resulted in significant 2D migration of the cell population of HaCaT cells (Figure 4A and B). On closer inspection of the coverslips it is evident that the cells had migrated off the coverslip on the left-hand side towards the magnet but not on the right-hand side (Fig. S4A and B ESI†). Furthermore, tracking of the nanoparticles by fluorescence clearly shows an increase in fluorescent signal off the coverslip on the left-hand side corresponding to this cell migration as well as a clear reduction in fluorescent density on the right hand side compared to the left, supporting the brightfield image and the cellular migration evident (Fig. S4C and D ESI†). Control

experiments of cells without nanoparticles (and no magnetic field) and cells in the presence of the magnetic field but without nanoparticles were also performed, with no directional bias and lower overall migration evident in both cases (Fig. S5A and B ESI†).

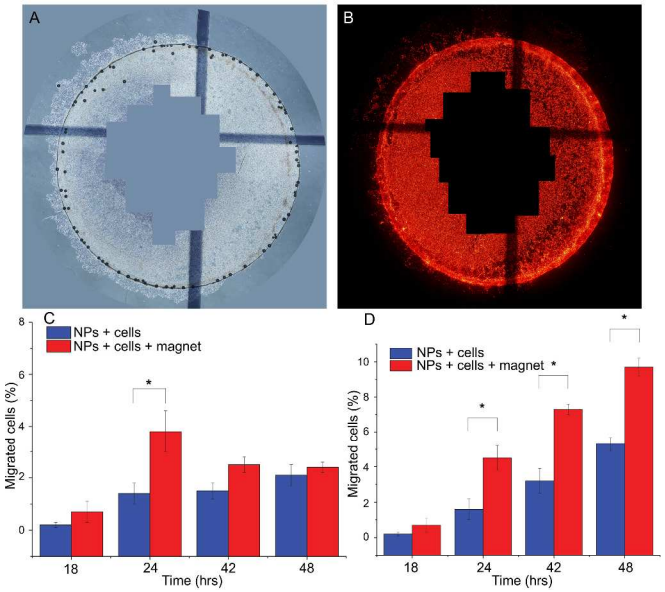

Fig. 4 (A & B) HaCaT cell migration towards the magnet (situated to the left of the coverslip) after 4 days in the presence of the magnetic field (0.6 T). (A) Stitched bright field image of the 10 mm coverslip depicting cell migration to the left and (B) visualisation of the Rhodamine B fluorescence from the internalised nanoparticles from the same coverslip. **Fig. 4 (C & D)** NIH-3T3 fibroblast migration in the presence of a 0.6 T field encouraging z-directed migration. (C) Cell counts (as a percentage of the total cells seeded) for each sample that have crossed the polycarbonate Transwell membrane at 18, 24, 42 and 48 h post plating of the cells, and (D) cumulative cell counts at each time point of the experiment. Data displayed as mean ± standard error from triplicate measurements at each time point. Significance was determined with ANOVA and Bonferroni–Dunn post hoc tests (significance of $P \leq 0.05$).

Fibroblast migration is also very important following a burn injury. In this study, fibroblast migration in the z-direction was assessed *in vitro* using a polycarbonate semi permeable Transwell membrane inserted into the well (See Fig S3B ESI† for experimental setup). As previously described, cells were incubated with the magnetic nanoparticles for 24 h before being seeded on a semi permeable polycarbonate Transwell membrane. Significantly higher migration was measured for the fibroblasts at 24 h following plating when compared to controls with nanoparticles but not in the presence of an external magnetic field. This significance was evident for each time point following 24 h out to 48 h for the cumulative cell counts in the experiment (Figure 4C and D). Control experiments comparing migration of cells without nanoparticles (control) in the presence of the magnetic field to that of cells with nanoparticles also produced a significant increase in nanoparticle enhanced migration compared to control cells at 24 h (Fig S6A, ESI†). However interestingly, looking at the same controls over cumulative cell counts this significance was evident at 24 and 42 h but not at the final time point of 48 h for the experiment (Fig S6B, ESI†). Previous studies have shown that the concentration of magnetic nanoparticles in cells has a maximum which occurs at approximately 24 h, and afterwards this concentration continuously declines.[27] However, despite this, the cause of this decline is not well understood. It could be due to different mechanisms like proliferation-dependent dilution, metabolic degradation, exocytosis or some combination of these processes resulting in the decrease of nanoparticle concentration.[28] The most likely mechanism in our case is also the simplest; cellular proliferation has resulted in the dilution of the magnetic nanoparticle concentration per cell. This dilution, lessens the control of the cells due to a reduction in the magnetic force exerted per cell over time and hence why at 48 h we see a lack of significance compared to control cells (Fig S6B, ESI†). For immediate future work, it is believed that translation to clinical practice will be best achieved with a small, circular magnet with a diameter similar to the wound size. This would best utilize the magnetic field to encourage cell migration to the wound site. In this proposed model, the area of greatest magnetic field strength lies at the edges of the circular permanent magnet; cells radially surround the wound site and will be encouraged to migrate inwards. Additionally, cells can be labelled with magnetic nanoparticles, injected into the blood stream and subsequently targeted to the wound site using this radial gradient. Clinically speaking, if we can increase the probability of cells attaching at the wound site as they travel through the blood stream, this could have beneficial wound healing outcomes and would be classed as a success.

Conclusions

In conclusion, we have developed a method for influencing the direction and speed of keratinocyte and fibroblast migration using an external magnetic field to attract cell internalised nanoparticles. This has implications in many biomedical fields, with the ability to exercise control over cells *in vivo*, a highly desirable outcome. The addition of the fluorescent Rhodamine B dye and magnetite nanoparticles, allow the cell-nanoparticle composites to be tracked and imaged on a range of different scales using 2 distinctly different modalities. This flexibility in tracking is important for regenerative medicine and cell therapy, with non-invasive MRI monitoring and whole-animal fluorescence helping to optimize *in vivo* transplantation procedures in terms of the number of required cells, the method or site of cell administration and the therapeutic time window.[29]

By providing directional cues to cells to enhance directional migration and consequently wound healing can become more efficient and potentially lead to improved patient outcomes. In a wound healing model, a new level of control over cell migration could lead to significantly faster healing and less subsequent complications. This will not only aid in skin wound healing, but could be applied to other cell types; for example, the guided cell migration of neurons could help bridge the nerve gap in spinal cord injuries and enhance the migration of Schwann cells into the injury site to promote axonal regeneration.[15] This study provides sound proof-of-concept for the enhancement of directionally induced cellular migration through the use of an applied magnetic field.

Acknowledgments

This work was funded by the Australian Research Council (ARC), and the National Health & Medical Research Council (NHMRC) of Australia. The authors acknowledge the Australian Microscopy & Microanalysis Research Facility at the Centre for Microscopy, Characterisation & Analysis, the University of Western Australia; funded by the University, State and Commonwealth Governments. LG is the beneficiary of a post-doctoral grant from the AXA

Research Fund. The cells for this work were graciously provided by the Fiona Wood Foundation.

Notes and references

a School of Chemistry and Biochemistry, M313, The University of Western Australia, 35 Stirling Highway, Crawley, WA, 6009, Australia.
b Fiona Wood Foundation, Burn Injury Research Unit, M509, The University of Western Australia, 35 Stirling Highway, Crawley, WA, 6009, Australia
c Biomagnetics Research Group, School of Physics, M013, The University of Western Australia, 35 Stirling Highway, Crawley, WA, 6009, Australia
d Department of Biomaterials and Bioinspired Materials, Instituto de Ciencia de Materiales de Madrid (ICMM)/CSIC, 28049 Madrid, Spain
e Departamento de Ciencia y Tecnología de Materiales y Fluidos, Universidad de Zaragoza, 50018, Zaragoza, Spain
f Burn Injury research Unit, School of Surgery, The University of Western Australia, 35 Stirling Highway, Crawley, WA, 6009, Australia
g Burns Service of Western Australia, Department of Health, Perth CBD, WA, 6000, Australia
* KSI: swaminatha.iyer@uwa.edu.au

† Electronic Supplementary Information (ESI) available: Nanoparticle characterisation, supporting experimental data, video time course study of cellular uptake of the nanoparticles and complete experimental details are all provided in the ESI, See DOI: 10.1039/c000000x/

1. P. Martin, *Science*, 1997, 276, 75-81.
2. R. F. Diegelmann and M. C. Evans, *Front Biosci*, 2004, 9, 283-289.
3. A. J. Ridley, M. A. Schwartz, K. Burridge, R. A. Firtel, M. H. Ginsberg, G. Borisy, J. T. Parsons and A. R. Horwitz, *Science*, 2003, 302, 1704-1709.
4. R. Clark, *The molecular and cellular biology of wound repair*, Springer, 1996.
5. R. J. Petrie, A. D. Doyle and K. M. Yamada, *Nature reviews Molecular cell biology*, 2009, 10, 538-549.
6. C. Carmona-Fontaine, H. Matthews and R. Mayor, *Cell adhesion & migration*, 2008, 2, 240-242.
7. L. L. Rodriguez and I. C. Schneider, *Integr. Biol.*, 2013, 5, 1306-1323.
8. X. Trepat and J. J. Fredberg, *Trends in cell biology*, 2011, 21, 638-646.
9. W. G. Williams and L. G. Phillips, in *Total burn care*, WB Saunders Company Ltd., 3rd edn., 1996.
10. I. Yannas and J. F. Burke, *Journal of biomedical materials research*, 1980, 14, 65-81.
11. M. G. Marks, C. Doillon and F. H. Silvert, *Journal of biomedical materials research*, 1991, 25, 683-696.
12. J. Bellemare, C. J. Roberge, D. Bergeron, C. A. Lopez-Vallé, M. Roy and V. J. Moulin, *The Journal of pathology*, 2005, 206, 1-8.
13. A. Ghahary and A. Ghaffari, *Wound Repair and Regeneration*, 2007, 15, S46-S53.
14. F. Bertorelle, C. Wilhelm, J. Roger, F. Gazeau, C. Ménager and V. Cabuil, *Langmuir*, 2006, 22, 5385-5391.
15. C. Riggio, M. P. Calatayud, C. Hoskins, J. Pinkernelle, B. Sanz, T. E. Torres, M. R. Ibarra, L. Wang, G. Keilhoff and G. F. Goya, *International journal of nanomedicine*, 2012, 7, 3155.
16. R. Schäfer, R. Bantleon, R. Kehlbach, G. Siegel, J. Wiskirchen, H. Wolburg, T. Kluba, F. Eibofner, H. Northoff and C. Claussen, *BMC cell biology*, 2010, 11, 22.
17. K. S. Midwood, L. V. Williams and J. E. Schwarzbauer, *The international journal of biochemistry & cell biology*, 2004, 36, 1031-1037.
18. C. W. Evans, M. Fitzgerald, T. D. Clemons, M. J. House, B. S. Padman, J. A. Shaw, M. Saunders, A. R. Harvey, B. Zdyrko, I. Luzinov, G. A. Silva, S. A. Dunlop and K. S. Iyer, *ACS Nano*, 2011, 5, 8640-8648.
19. T. D. Clemons, H. M. Viola, M. J. House, K. S. Iyer and L. C. Hool, *ACS Nano*, 2013, 7, 2212-2220.
20. J. Harrison, C. A. Bartlett, G. Cowin, P. K. Nicholls, C. W. Evans, T. D. Clemons, B. Zdyrko, I. A. Luzinov, A. R. Harvey, K. S. Iyer, S. A. Dunlop and M. Fitzgerald, *Small*, 2012, 8, 1579-1589.
21. L. Gutiérrez, M. Morales and F. J. Lázaro, *Physical Chemistry Chemical Physics*, 2014, 16, 4456-4464.
22. A. López, L. Gutiérrez and F. J. Lázaro, *Physics in Medicine and Biology*, 2007, 52, 5043.
23. L. Gutiérrez, R. Mejías, D. Barber, S. Veintemillas-Verdaguer, C. Serna, F. Lázaro and M. Morales, *Journal of Physics D: Applied Physics*, 2011, 44, 255002.
24. L. Gutiérrez, M. Vujić Spasić, M. U. Muckenthaler and F. J. Lázaro, *Biochimica et Biophysica Acta - Molecular Basis of Disease*, 2012, 1822, 1147-1153.
25. M. Iwasaka and S. Ueno, *J. Appl. Phys.*, 2005, 97.
26. Y. Nakaoka, R. Takeda and K. Shimizu, *Bioelectromagnetics*, 2002, 23, 607-613.
27. M. Colombo, S. Carregal-Romero, M. F. Casula, L. Gutierrez, M. P. Morales, I. B. Bohm, J. T. Heverhagen, D. Prosperi and W. J. Parak, *Chemical Society Reviews*, 2012, 41, 4306-4334.
28. E. M. Bachelder, T. T. Beaudette, K. E. Broaders, S. E. Paramonov, J. Dashe and J. M. Fréchet, *Molecular pharmaceutics*, 2008, 5, 876-884.
29. S. Kubinova and E. Sykova, *Minim. Invasive Ther. Allied Technol.*, 2010, 19, 144-156.